JCTC Journal of Chemical Theory and Computation

Article

pubs.acs.org/JCTC

Accurate Theoretical Description of the ^1L_a and ^1L_b Excited States in Acenes Using the All Order Constricted Variational Density Functional Theory Method and the Local Density Approximation

Mykhaylo Krykunov,*[,†] Stefan Grimme,[‡] and Tom Ziegler[†]

[†]Department of Chemistry, University of Calgary, University Drive 2500, Calgary, Alberta, Canada T2N 1N4

[‡]Mulliken Center for Theoretical Chemistry, Institut für Physikalische und Theoretische Chemie der Universität Bonn, Beringstr. 4, D-53115, Germany

ABSTRACT: We present the results of calculations on the vertical singlet ^1L_a and ^1L_b excitation energies in acenes within time dependent density functional theory (TDDFT), second order constricted variational DFT (CV(2)-DFT), and all order constricted variational DFT (CV(∞)-DFT) using the local density approximation LDA(VWN). For the linear acenes it is shown that the application of the Tamm−Dancoff (TD) approximation to TDDFT (TDDFT-TD) substantially improves the agreement with experiment compared to pure TDDFT. This improvement leads to the correct ordering of the ^1L_a and ^1L_b excitation energies in naphthalene. As TDDFT-TD is equivalent to the second order CV(2)-TD method one might hope for further improvements by going to all orders in CV(∞)-TD. Indeed, for linear acenes the application of the CV(∞)-TD method brings the agreement with experiment to within 0.1 eV for both types of excitations using the simple LDA functional. The CV(∞)-TD method based on LDA is also shown to be accurate for 15 nonlinear acenes with root-mean-square deviations of 0.24 eV for ^1L_a and 0.17 eV for ^1L_b.

1. INTRODUCTION

A number of π-conjugated systems in the form of organic dyes have recently attracted considerable attention as possible candidates that might be incorporated into dye-sensitized solar cells. To devise the optimal cell, it would be very helpful to have an accurate theoretical method that could search for good candidates among the many possible dyes in a both efficient and accurate manner. In order to establish such a method, it is also necessary to have a set of benchmarks among $\pi \rightarrow \pi^*$ excitation energies in extended π-conjugated systems. Fortunately, the singlet ^1L_a and ^1L_b excitations in linear polyacenes represent such a set of benchmark data as they have been studied extensively both experimentally and theoretically. Here the acenes consist of a number (n_r) of fused benzene rings.

The distinct properties[1] of the ^1L_a and ^1L_b states for the linear acenes have already been described in the literature.[2,3] Essentially, the ^1L_a (or $^1B_{2u}$ when the x-axis corresponds to the long molecular axis) state is dominated by a single electron transition HOMO → LUMO, while the ^1L_b (or $^1B_{3u}$) state results from a combination of HOMO − 1 → LUMO and HOMO → LUMO + 1 transitions. Further, excitations to ^1L_a ($^1B_{2u}$) are short axis polarized with high intensity whereas the transitions to ^1L_b ($^1B_{3u}$) are long axis polarized with low intensity, Table 1. The relative ordering of the ^1L_a and ^1L_b states is size dependent. Thus, for naphthalene with two rings the ^1L_b state is below ^1L_a in energy while for the other linear acenes the ordering is opposite although the splitting is very small for anthracene with n_r =3. Both states drop in energy with increasing n_r but the drop is largest for ^1L_a, see Table 1 and Figure 1.

It was previously reported[2,3] that TDDFT[4−7] incorrectly predicts the crossing point of the ^1L_a and ^1L_b states in linear polyacenes with both semilocal and hybrid functionals. Further, the computed TDDFT excitation energies for ^1L_a relative to ^1L_b are in poor agreement with experiment throughout the range n_r = 2, 6.[8,9] Promising alternative methods are the DFT/MRCI approach[11,12] and TDDFT schemes based on long-range corrected (LRC) functionals.[13−16] The DFT/MRCI approach is quite accurate but not a "black box" method like the TDDFT scheme. This makes it difficult to use DFT/MRCI in screening type applications. The LRC methods show some improvement for ^1L_a but not for ^1L_b.[16] Further, the optimal range separation parameter(s) must be determined for each molecule. A more recent promising approach is double-hybrid density functional theory.[20−25] This scheme has to date provided the most balanced description of the linear acenes.[25] Unfortunately, these double hybrids are limited to low valence excitations due to the inherent perturbative corrections.[26]

Some of us have recently put forward[27] the constricted variational density functional theory (CV-DFT) as a possible improvement of adiabatic TDDFT. The new theory is in its simplest second order formulation (CV(2)-DFT) identical to adiabatic TDDFT after use has been made of the popular Tamm−Dancoff approximation.[28] However, the method can be extended to all orders in the variational parameters (CV(∞)-DFT). It has been shown in a recent study[27] that the $\pi \rightarrow \pi^*$ transitions in conjugated hydrocarbons are described reasonably well within the CV(∞)-DFT scheme. An average deviation from experiment is approximately 0.3 eV for both semilocal and hybrid functionals.

We shall here first assess the ability of our newly developed constricted variational density functional theory (CV-DFT)[27] to describe the excited states in linear polyacenes, as a first step in an attempt to establish an inexpensive method that ultimately can

Received: May 11, 2012
Published: August 23, 2012

dx.doi.org/10.1021/ct300372x | J. Chem. Theory Comput. 2012, 8, 4434−4440

Table 1. LDA(VWN)-Based $^1L_a(^1B_{2u})$ and $^1L_b(^1B_{3u})$ Singlet Excitation Energies (in eV) for Acenes with CV(2)-TD and TDDFT

	expt[c]			CV(2)-TD[d]		f^b			TDDFT		
n_r[e]	$^1B_{2u}$	$^1B_{3u}$	ΔE^a	$^1B_{2u}$	$^1B_{3u}$	ΔE^a	$^1B_{2u}$	$^1B_3$	$^1B_{2u}$	$^1B_{3u}$	ΔE^a
2	4.66	4.13	−0.53	4.27	4.21	0.06	0.0545	0.0000	4.07	4.41	0.34
3	3.60	3.64	−0.04	3.13	3.60	−0.47	0.0578	0.0003	2.91	3.78	−0.87
4	2.88	3.39	−0.51	2.38	3.21	−0.83	0.0533	0.0013	2.15	3.35	−1.20
5	2.37	3.12	−0.75	1.86	2.94	−1.08	0.0469	0.0033	1.62	3.08	−1.46
6	2.02	2.87	−0.85	1.47	2.74	−1.27	0.0399	0.0071	1.22	2.86	−1.64
rmsd				0.49	0.13				0.71	0.14	

[a] $\Delta E = \Delta E(^1B_{2u}) - \Delta E(^1B_{3u})$. [b] Oscillator strength. [c] Reference 34. [d] Tamm-Dancoff approximation. [e] Number of rings.

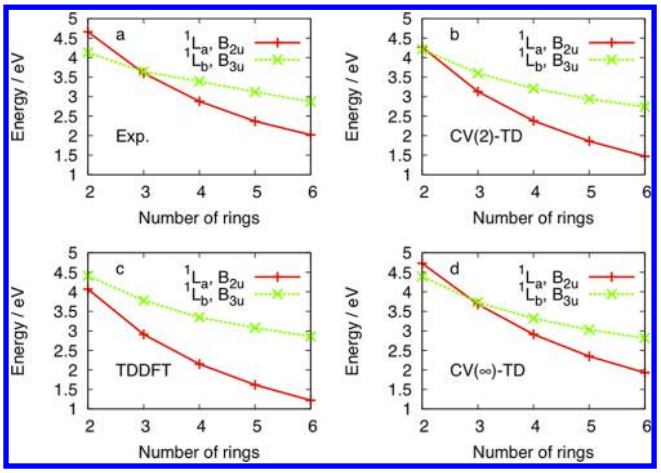

Figure 1. Excitation energies for the ^1L_a and ^1L_b transitions in linear acenes as a function of the number of rings according to (a) experiment, (b) CV(2)-TD, (c) TDDFT, and (d) CV(∞)-TD.

help in the design of light-harvesting devices. It is further our objective to demonstrate that quite accurate results can be obtained for our test set even with the simple LDA functional if one goes beyond the simple second order approximation inherent in TDDFT and incorporate terms to all orders in the variational parameters, as it is done in CV(∞)-DFT. Our work is a continuation of a previous study in which we demonstrated that LDA can be used to describe charge transfer transitions within the constricted variational DFT method.[29] We shall finally extend the scope of our investigation to include the ^1L_a and ^1L_b excitations in 15 nonlinear polyacenes.

2. COMPUTATIONAL METHOD AND COMPUTATIONAL DETAILS

2.1. Constricted Variational Density Functional Theory. In CV(n)-DFT, we carry out a unitary transformation among occupied $\{\phi_i; i = 1,\text{occ}\}$ and virtual $\{\phi_a; a = 1,\text{vir}\}$ ground state orbitals

$$Y\begin{pmatrix}\phi_{\text{occ}}\\ \phi_{\text{vir}}\end{pmatrix} = e^{\mathbf{U}}\begin{pmatrix}\phi_{\text{occ}}\\ \phi_{\text{vir}}\end{pmatrix} = \left(\sum_{m=0}^{m=\infty}\frac{\mathbf{U}^m}{m!}\right)\begin{pmatrix}\phi_{\text{occ}}\\ \phi_{\text{vir}}\end{pmatrix} = \begin{pmatrix}\phi'_{\text{occ}}\\ \phi'_{\text{vir}}\end{pmatrix} \quad (1)$$

with the summation over m in eq 1 truncated at $m = n$. Thus, the resulting orbitals will be orthonormal to order n in $\mathbf{U}$. Here ϕ_{occ} and ϕ_{vir} are concatenated column vectors consisting of the sets $\{\phi_i; i = 1,\text{occ}\}$ and $\{\phi_a; a = 1,\text{vir}\}$ of occupied and virtual ground state orbitals, respectively, whereas ϕ'_{occ} and ϕ'_{vir} are concatenated column vectors containing the resulting sets $\{\phi'_i; i = 1,\text{occ}\}$ and $\{\phi'_a; a = 1,\text{vir}\}$ of occupied and virtual excited state orbitals, respectively. The unitary transformation matrix Y is in eq 1 expressed in terms of a skew symmetric matrix U as

$$\begin{aligned} Y &= e^U \\ &= I + U + \frac{U^2}{2} + \ldots \\ &= \sum_{m=0}^{\infty}\frac{U^m}{m!} \\ &= \sum_{m=0}^{\infty}\frac{(U^2)^m}{2m!} + U\sum_{m=0}^{\infty}\frac{(U^2)^m}{(2m+1)!} \end{aligned} \quad (2)$$

Here $U_{ij} = U_{ab} = 0$ where "i,j" refers to the occupied set $\{\phi_i; i = 1,\text{occ}\}$ whereas "a,b" refers to $\{\phi_a; a = 1,\text{vir}\}$. Further, U_{ai} are the variational mixing matrix elements that combine virtual and occupied ground state orbitals in the excited state with $U_{ai} = -U_{ia}$. The new occupied set $\{\phi'_i; i = 1,\text{occ}\}$ provides us with the excited state KS-determinant $\Psi' = |\phi'_1\phi'_2\ldots\phi'_i\phi'_j\ldots\phi'_n|$ from which we can express the corresponding spin and space density matrices s' and ρ'. These matrices allow us subsequently to express the Kohn−Sham energy of Ψ' as $E[\rho'^+, \rho'^-]$ where $\rho'^+ = \rho'/2 + s'/2$ and $\rho'^- = \rho'/2 - s'/2$.[27]

In CV(2)-DFT the summation in eq 1 is carried out to $m = 2$ so that the corresponding orbitals are orthonormal up to second order in U. From that $E[\rho'^+, \rho'^-]$ is expressed to second order in U from the second order density and spin matrices as $E[\rho^{(2)+}, \rho^{(2)-}]$. A subsequent optimization of $E[\rho^{(2)+}, \rho^{(2)-}]$ under the constraint[27] that exactly one electron is moved from the density space spanned by $\{\phi_i; i = 1,\text{occ}\}$ to the space spanned by $\{\phi_a; a = 1,\text{vir}\}$ affords after applying the Tamm−Dancoff approximation[28] the eigenvalue equation

$$\mathbf{AU}^{(I)} = \lambda^{(I)}U^{(I)} \quad (3)$$

where

$$A_{ai,bj} = \delta_{ab}\delta_{ij}(\varepsilon_a - \varepsilon_i) + K_{ai,bj} \quad (4)$$

We shall refer to the CV(2)-DFT method in which we have used the Tamm−Dancoff approximation[28] as simply CV(2)-TD.

In eq 4 ε_a and ε_i refer to ground state orbital energies. Further, $K_{ai,bj} = K^C_{ai,bj} + K^{XC}_{ai,bj}$ where

$$K^C_{ai,bj} = \iint \phi_a(1)\phi_i(1)\frac{1}{r_{12}}\phi_b(2)\phi_j(2)\,\mathrm{d}v_1\mathrm{d}v_2 \quad (5)$$

whereas

$$K^{XC(HF)}_{ai,bj} = -\int\int \phi_a(1)\phi_i(2)\frac{1}{r_{12}}\phi_b(1)\phi_j(2)\,\mathrm{d}v_1\mathrm{d}v_2 \quad (6)$$

for Hartree−Fock exchange correlation and

dx.doi.org/10.1021/ct300372x | J. Chem. Theory Comput. 2012, 8, 4434−4440

$$K_{ai,bj}^{XC(KS)} = \int\int \phi_a(1)\phi_i(1)f(1)\phi_b(1)\phi_j(1)\,\mathrm{d}v_1\mathrm{d}v_2 \tag{7}$$

for KS exchange correlation. In eq 7 f is the energy kernel. We note that an expression similar to eq 3 can be derived[4] from adiabatic TDDFT after application of the Tamm−Dancoff approximation.[28] Thus adiabatic TDDFT-TD based on response theory and CV(2)-TD based on variation theory are mathematically equivalent.

After solving eq 3 we apply the resulting **U** to eqs 1 and 2 in an all order unitary transformation from which we can obtain $E[\rho^{(\infty)+}, \rho^{(\infty)-}]$ corresponding to CV(∞)-DFT. In general, in CV(n)-DFT we use the **U** from eq 3 to express $E[\rho^{(n)+}, \rho^{(n)-}]$. It is also possible to determine **U** directly by optimizing $E[\rho^{(n)+}, \rho^{(n)-}]$. In that case we talk about SCF-CV(n)-DFT.[27] We shall here only be interested in CV(n)-DFT as we want the simplest possible theory that can describe $\pi \rightarrow \pi^*$ excitation in dyes. However, the $\pi \rightarrow \pi^*$ excitations in conjugated hydrocarbons have been studied extensively by SCF-CV(n)-DFT.[27]

We shall now turn to a discussion of how we construct the proper energy expression for excited singlet states originating from a closed shell ground state. Considering first a spin-conserving transition from a close shell ground state and assume without loss of generality that the transition takes place in the α-manifold. In that case we can write the occupied excited state KS-orbitals generated from the unitary transformation of eq 1 as[27]

$$\phi'_i = \cos[\eta\gamma_i]\phi_i^{o_\alpha} + \sin[\eta\gamma_i]\phi_i^{v_\alpha};\ i = 1,\ \mathrm{occ}/2 \tag{8}$$

and

$$\phi'_i = \phi_i;\ \ i = 1,\ \mathrm{occ}/2 + 1,\ \mathrm{occ} \tag{9}$$

whereas the corresponding KS-determinant is given by

$$\Psi_M = |\phi'_1\phi'_2...\phi'_i\phi'_j...\phi'_n| \tag{10}$$

Here Ψ_M represents a mixed spin-state[42] that is half singlet and half triplet. Further, $\gamma_i(i = 1,\mathrm{occ}/2)$ is a set of eigenvalues to

$$(\mathbf{V}^{\alpha\alpha})^{+}\mathbf{U}^{\alpha\alpha}\mathbf{W}^{\alpha\alpha} = \mathbf{1}\gamma \tag{11}$$

where γ is a diagonal matrix of dimension occ/2 whereas $\mathbf{U}^{\alpha\alpha}$ is the part of the U matrix that runs over the occupied $\{\phi_i;\ i = 1,\mathrm{occ}/2\}$ and virtual $\{\phi_a;\ i = 1,\mathrm{vir}/2\}$ ground state orbitals of α-spin.[27,49] Further

$$\phi_i^{o_\alpha} = \sum_{j}^{\mathrm{occl2}} (W^{\alpha\alpha})_{ji}\phi_j \tag{12}$$

and

$$\phi_i^{v_\alpha} = \sum_{a}^{\mathrm{virl2}} (V^{\alpha\alpha})_{ai}\psi_a \tag{13}$$

Finally, η is determined in such a way that $\sum_{i=1}^{\mathrm{occ}/2}\sin^2[\eta\gamma_i] = 1$, corresponding to the constraint that exactly one electron charge is involved in the transition. The orbitals defined in eqs 12 and 13 have been referred to as natural transition orbitals (NTOs)[50] since they give a more compact description of the excitations than the canonical orbitals. Thus, a transition that involves several $i \rightarrow a$ replacements among canonical orbitals can often be described by a single replacement $\phi_i^{o_\alpha} \rightarrow \phi_i^{\nu_\alpha}$ in terms of NTOs. We note again that the set in eq 8 is obtained from the unitary transformation in eq 1 among the occupied $\{\phi_i;\ i = 1,\mathrm{occ}/2\}$ and virtual $\{\phi_a;\ i = 1,\mathrm{vir}/2\}$ ground state orbitals of α-spin with **U** represented by $\mathbf{U}^{\alpha\alpha}$.

For a spin-flip transition from a closed shell ground state the unitary transformation in eq 1 among the occupied ground state orbitals $\{\phi_i;\ i = 1,\mathrm{occ}/2\}$ of α-spin and the virtual ground state orbitals $\{\phi_a;\ i = \mathrm{vir}/2 + 1,\mathrm{vir}\}$ of β-spin yields the occupied excited state orbitals

$$\phi''_i = \cos[\eta\gamma'_i]\phi_i^{o_\alpha} + \sin[\eta\gamma'_i]\phi_i^{v_\beta};\ \ i = 1,\ \mathrm{occ}/2 \tag{14}$$

and

$$\phi''_i = \phi_i;\ \ i = \mathrm{occ}/2 + 1,\ \mathrm{occ} \tag{15}$$

whereas the corresponding KS-determinant is given by

$$\Psi_T = |\phi'_1\phi'_2...\phi'_i\phi'_j...\phi'_n| \tag{16}$$

Here Ψ_T represents a triplet state. Further, $\gamma'_i(i = 1,\mathrm{occ}/2)$ are the eigenvalues to

$$(\mathbf{V}^{\beta\alpha})^{+}\mathbf{U}^{\beta\alpha}\mathbf{W}^{\beta\alpha} = \mathbf{1}\gamma' \tag{17}$$

where $\mathbf{U}^{\beta\alpha}$ is the part of **U** that runs over the virtual ground state orbitals of β-spin and occupied ground state orbitals of α-spin. Finally

$$\phi_i^{o_\alpha} = \sum_{j=1}^{\mathrm{occ}/2} (W^{\beta\alpha})_{ji}\phi_j \tag{18}$$

and

$$\phi_i^{v_\beta} = \sum_{a=\mathrm{vir}/2+1}^{a=\mathrm{vir}} (V^{\beta\alpha})_{ai}\psi_a \tag{19}$$

With the energy of Ψ_T given by E_T and that of Ψ_M as E_M, we can write the singlet transition energy as[42]

$$\Delta E_S = 2E_M - E_T - E_0 \tag{20}$$

provided that $\mathbf{U}^{\alpha\alpha} = \mathbf{U}^{\beta\alpha}$. This implies that $\mathbf{V}^{\alpha\alpha} = \mathbf{V}^{\beta\alpha}$; $W^{\alpha\alpha} = W^{\beta\alpha}$, and $\gamma = \gamma'$. Further, $\phi_i^{o_\alpha}$ of eqs 8 and 14 become identical as do the spatial parts of $\phi_i^{v_\alpha}$ and $\phi_i^{v_\beta}$ in the same two equations. In CV(∞)-DFT use is made of the $U^{\beta\alpha}$ matrix obtained from a CV(2)-TD singlet calculation. Straightforward manipulations[27] allow us finally to write down the singlet transition energy in a compact and closed form as

$$\begin{aligned}\Delta E_S = &\sum_{i=1}^{\mathrm{occ}/2} \sin^2[\eta\gamma_i](\varepsilon_{i^{v_\alpha}} - \varepsilon_{i^{o_\alpha}}) \\ &+ \frac{1}{2}\sum_{i=1}^{\mathrm{occ}/2}\sum_{j=1}^{\mathrm{occ}/2} \sin^2[\eta\gamma_j]\sin^2[\eta\gamma_i](K_{i^{o_\alpha}i^{v_\alpha}j^{o_\alpha}j^{o_\alpha}} \\ &+ K_{i^{v_\alpha}i^{v_\alpha}j^{v_\alpha}j^{v_\alpha}} - 2K_{i^{v_\alpha}i^{v_\alpha}j^{o_\alpha}j^{o_\alpha}} + K_{\bar{i}^{v_\beta}\bar{i}^{v_\beta}\bar{j}^{o_\alpha}\bar{j}^{o_\alpha}}] \\ &\sum_{i=1}^{\mathrm{occ}/2}\sum_{j=1}^{\mathrm{occ}/2} \sin[\eta\gamma_j]\cos[\eta\gamma_j]\sin[\eta\gamma_i]\cos[\eta\gamma_i] \\ &(2K_{i^{o_\alpha}i^{v_\alpha}j^{o_\alpha}j^{v_\alpha}} - K_{i^{o_\alpha}\bar{i}^{v_\beta}\bar{j}^{o_\alpha}\bar{j}^{v_\beta}})\end{aligned} \tag{21}$$

Here the indices i^{o_α}, j^{o_α}, i^{v_α}, and j^{v_α} refer to α-spin orbitals with the spatial parts $\phi_i^{o_\alpha}$, $\phi_j^{o_\alpha}$, $\phi_i^{v_\alpha}$, and $\phi_j^{v_\alpha}$, respectively. Likewise, the indices $\bar{i}^{o_\beta}$, $\bar{j}^{o_\beta}$, $\bar{i}^{v_\beta}$, and $\bar{j}^{v_\beta}$ refer to β-spin orbitals with the spatial parts $\phi_i^{o_\beta}$, $\phi_j^{o_\beta}$, $\phi_i^{v_\beta}$, and $\phi_j^{v_\beta}$, respectively. In deriving eq 21 we have applied the Tamm−Dancoff approximation[28] by neglecting integrals of the type $K_{i^{o_\alpha}i^{v_\alpha}j^{v_\alpha}j^{o_\alpha}}$ in the third term on the right-hand side of eq 21 as well as numerically very small contributions that are third order in $\sin[\eta\gamma_i]$. These approximations are introduced to ensure that eq 21 for excitations that are described by several

displacements converge to the CV(2)-TD expression for a singlet transition, as we shall discuss shortly. The expression for the corresponding triplet transition energy reads

$$\Delta E_T = \sum_{i=1}^{occ/2} \sin^2[\eta\gamma_i](\varepsilon_{i^{\alpha}} - \varepsilon_{i^{\alpha}}) + \frac{1}{2}\sum_{i=1}^{occ/2}\sum_{j=1}^{occ/2} \sin^2[\eta\gamma_j]\sin^2[\eta\gamma_i](K_{i^{\alpha}i^{\alpha}j^{\alpha}j^{\alpha}} + K_{\bar{i}^{\beta}\bar{i}^{\beta}\bar{j}^{\beta}\bar{j}^{\beta}} - K_{\bar{i}^{\beta}\bar{i}^{\beta}j^{\alpha}j^{\alpha}}] \sum_{i=1}^{occ/2}\sum_{j=1}^{occ/2} \sin[\eta\gamma_j]\cos[\eta\gamma_j]\sin[\eta\gamma_i]\cos[\eta\gamma_i] - K_{i^{\alpha}\bar{i}^{\beta}j^{\alpha}\bar{j}^{\beta}} \quad (22)$$

We shall from now on refer to CV(∞)-DFT calculations in which eqs 21 and 22 are used as CV(∞)-TD. Please note that, for single displacement transitions where $\eta\gamma_j = \pi/2$ for $j = i$ and $\eta\gamma_j = 0$ for $j \neq i$, we get the same energy whether the TD-approximation is used or not since only the first and second term in eq 22 contributes to ΔE_S.

2.2. Computational Details. All calculations have been performed with the developer's version of the Amsterdam Density Functional (ADF) package. The Slater-type basis supplied by ADF[30] version 2010 was of triple-ζ quality[31] with an additional set of polarized functions (TZP). From extensive TDDFT studies[23−25] on dyes, we estimate that our excitation energies are within 0.1−0.2 eV of those obtained by a converged basis set. Use was made of the local density approximation LDA(VWN)[32] in the parametrization due to Vosko, Wilk, and Nusair. For the calculation of the exact Hartree−Fock exchange integrals over Slater-type orbitals, a double fitting procedure has been employed.[33] All ground state structures were adopted from the work of Richard and Herbert.[16]

3. RESULTS AND DISCUSSION

We present in Table 1 the calculated $^1A_{1g} \rightarrow {}^1B_{2u}$ and $^1A_{1g} \rightarrow {}^1B_{3u}$ excitation energies $\Delta E(^1B_{2u})$ and $\Delta E(^1B_{3u})$, respectively, for linear acenes employing the TDDFT and CV(2)-TD methods in conjunction with the LDA(VWN) functional. Also shown are the calculated oscillatory strengths of the two excitations. Extensive studies[16] have shown that the $^1A_{1g} \rightarrow {}^1B_{2u}$ transition essentially can be represented by the HOMO → LUMO promotion whereas $^1A_{1g} \rightarrow {}^1B_{3u}$ is a nearly equal mixture of the HOMO − 1 → LUMO and HOMO → LUMO + 1 promotions.

Excitation energies (ΔE_S) due to transitions from a closed shell ground state to a singlet excited state have in CV(2)-TD the simple form[27]

$$\Delta E_S = \sum_{a}^{vir/2}\sum_{i}^{occ/2} U_{ai}U_{ai}(\varepsilon_a - \varepsilon_i) + 2\sum_{a,b}^{vir/2}\sum_{i,j}^{occ/2} U_{ai}U_{ai}K_{ai,bj} - \sum_{a,b}^{vir/2}\sum_{i,j}^{occ/2} U_{a\bar{i}}U_{b\bar{j}}K_{a\bar{i},b\bar{j}} \quad (23)$$

Here superscript "bars" refer to orbitals of β-spin whereas i,a without bars represent α-orbitals. The corresponding energies in TDDFT have a somewhat more complex form[4] but depend again on $(\varepsilon_a - \varepsilon_I)$, $K_{ai,bj}$, $K_{a\bar{i},b\bar{j}}$, and $\mathbf{U}$.

It follows from Table 1 and Figure 1a that the experimental energy gap $\Delta E = \Delta E(^1B_{2u}) - \Delta E(^1B_{3u})$ starts out positive at naphthalene ($n_r = 2$) with $\Delta E = 0.53$ eV before turning negative at anthracene ($n_r = 3$) where $\Delta E = -0.04$ eV. For larger linear acenes ΔE becomes increasingly negative reaching $\Delta E = -0.85$ eV at hexacene. Thus, experimentally, $\Delta E(^1B_{2u})$ is seen to drop faster in energy than $\Delta E(^1B_{3u})$.

The ordering of the calculated CV(2)-TD excitation energies based on LDA(VWN) is correct for naphthalene as well as for all other linear acenes; however, the gap differs from the experimental ΔE by almost 0.4 eV for naphthalene, anthracene, and, hexacene. This difference is smaller for napthacene and pentacene, Table 1 and Figure 1b. It can be seen that the main contribution to this deviation comes from the underestimation of $\Delta E(^1B_{2u})$. Thus, the root-mean-square deviation (rmsd) value for $\Delta E(^1B_{2u})$ is 0.49 eV, while it is only 0.13 eV for $\Delta E(^1B_{3u})$.

As for the TDDFT results based on LDA(VWN), the deviation from the experimental gaps is larger in absolute terms and the calculated ΔE has the wrong sign for naphthalene, Table 1 and Figure 1c. It happens, because the $\Delta E(^1B_{2u})$ values for TDDFT are lower than those for CV(2)-TD while the $\Delta E(^1B_{3u})$ estimates for TDDFT are higher than for CV(2)-TD. As a result, the rmsd value for $\Delta E(^1B_{2u})$ increases for TDDFT by approximately 0.2 eV and reaches 0.71 eV. On the other hand, on average the TDDFT estimate of $\Delta E(^1B_{3u})$ is as accurate as for CV(2)-TD. Thus, the TDDFT $\Delta E(^1B_{3u})$ values for napthacene, pentacene, and hexacene are closer to experiment than those due to CV(2)-TD while the opposite is true for naphthalene and anthracene. The rmsd value for TDDFT is 0.14 eV compared to 0.13 eV for CV(2)-TD, Table 1.

It follows from the discussion given above that neither CV(2)-TD nor TDDFT are able to give a quantitative description of ΔE as a function of n_r with LDA, in line with previous TDDFT studies[2,3,8,9] using both pure density functionals and hybrids. The source of the error is in all cases primarily $\Delta E(^1B_{2u})$ that is too low compared to experiment. However, $\Delta E(^1B_{3u})$ is in addition seen to be slightly too high.

We have in order to analyze our findings further displayed the orbital energy dependent part

$$\Delta\varepsilon = \sum_{a}^{vir/2}\sum_{i}^{occ/2} U_{ai}U_{ai}(\varepsilon_a - \varepsilon_i) \quad (24)$$

in the expression for ΔE_S according to CV(2)-TD, eq 23, along with the K-integral dependent part $\Delta E_S - \Delta\varepsilon$ in Table 2 and Figure 2a,b as a function of n_r for LDA in the case of $\Delta E(^1B_{3u})$ and $\Delta E(^1B_{2u})$. We see that both the slope and the absolute value of $\Delta E(^1B_{3u})$ and $\Delta E(^1B_{2u})$ are determined by $\Delta\varepsilon$ and that the contributions to ΔE_S from the K-integrals amount to 0.3 eV for

Table 2. Contributions from Orbital Energies and K-Integrals to the Calculated Excitation Energies (eV) for CV(2)-TD[d] and LDA

	calcd $^1B_{2u}$		calcd $^1B_{3u}$	
n_r[c]	$\Delta\varepsilon$[a]	$(\Delta E_S - \Delta\varepsilon)$[b]	$\Delta\varepsilon$	$\Delta E_S - \Delta\varepsilon$
2	3.95	0.32	4.14	0.07
3	2.83	0.30	3.55	0.05
4	2.11	0.27	3.16	0.05
5	1.60	0.26	2.90	0.04
6	1.23	0.24	2.71	0.03

[a]Orbital energy contributions to the excitation energies, see eqs 25 and 26. [b]Contributions from K-integrals to the excitation energies. [c]Number of rings. [d]Tamm−Dancoff approximation.

dx.doi.org/10.1021/ct300372x | J. Chem. Theory Comput. 2012, 8, 4434−4440

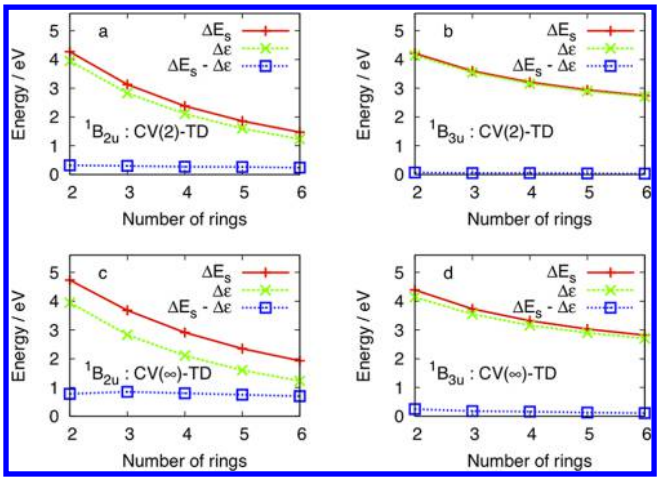

Figure 2. Contributions from orbital energies and K-integrals to the calculated excitation energies (eV) in linear acenes for CV(2)-TD with respect to (a) $^1B_{2u}$ (^1L_a) and (b) $^1B_{3u}$ (^1L_b) as well as CV(∞)-TD with respect to (c) $^1B_{2u}$ (^1L_a) and (d) $^1B_{3u}$ (^1L_b).

$\Delta E(^1B_{2u})$ and 0.1 eV for $\Delta E(^1B_{3u})$, where both contributions diminish slightly with n_r.

Turning now to the CV(∞)-DFT scheme we note that the excitation energy in eq 21 for a transition that involves a single promotion $i \rightarrow a$ such as $^1A_{1g} \rightarrow {}^1B_{2u}$ has the simple form[27]

$$\Delta E_S^{CV(\infty)}(i \rightarrow a) = \varepsilon_a - \varepsilon_i + \frac{1}{2}K_{aaaa} + \frac{1}{2}K_{iiii} - 2K_{aaii} + K_{i\bar{a}i\bar{a}} \quad (25)$$

.Here i is the HOMO and a the LUMO. For CV(2) we obtain for the same transition according to eq 23

$$\Delta E_S^{CV(2)}(i \rightarrow a) = \varepsilon_a - \varepsilon_i + 2K_{aiai} - K_{i\bar{a}i\bar{a}} \quad (26)$$

.

For HF these two expressions are identical[27] since $K_{aaaa} = K_{iiii} = 0$ and $K_{aiai} = -K_{aaii}$. However, for any of the popular functionals this is not the case. Thus, the two expressions will give rise to different excitation energies for the same functional, as we shall see. For transitions consisting of two or more promotions such as $^1A_{1g} \rightarrow {}^1B_{3u}$, the expression of eq 21 for $\Delta E_S^{CV(\infty)}$ contains contributions that are second and fourth order in sine function. The contributions from the latter terms diminish rapidly in magnitude with the number of promotions due to the constraint $\sum_{i=1}^{occ/2}\sin^2[\eta\gamma_i] = 1$. Thus, for four equally participating promotions with $\sin^2[\eta\gamma_i] = 1/4$ ($i = 1, 4$), the fourth order prefactors $\sin^4[\eta\gamma_i]$ are small (1/16) and the terms in eq 21 to second order in sine will dominate since $\sin^2[\eta\gamma_i] = 1/4$ ($i = 1, 4$). In the limit of many more participating promotions from eq 21, this will converge to 23.

It follows from Table 3 and Figure 1d that the CV(∞)-DFT results using LDA are in excellent agreement with experiment for both $\Delta E(^1B_{3u})$ and $\Delta E(^1B_{2u})$ throughout the range of linear acenes. The rmsd for $\Delta E(^1B_{2u})$ is 0.06 eV whereas that for $\Delta E(^1B_{3u})$ is 0.13 eV. Thus, CV(∞)-DFT clearly represents an improvement over TDDFT and CV(2)-TD for LDA. The improvement is as anticipated most noticeable for $\Delta E(^1B_{2u})$ where the rmsd was 0.71 eV for TDDFT and 0.49 eV for CV(2)-TD. For $\Delta E(^1B_{3u})$, all three methods have a similar rmsd.

The magnitude of $^1/_2K_{aaaa} + {}^1/_2K_{iiii} - 2K_{aaii} + 2K_{ii\bar{a}\bar{a}}$ from eq 25 is given in Table 4 and Figure 2c for $^1B_{2u}$ as $\Delta E(^1B_{2u}) -$

Table 3. CV(∞)-TD Singlet Excitation Energies (in eV) for Linear Acenes with LDA

	expt[b]			LDA		
no. rings	$^1B_{2u}$	$^1B_{3u}$	ΔE^a	$^1B_{2u}$	$^1B_{3u}$	ΔE^a
2	4.66	4.13	0.53	4.73	4.39	0.34
3	3.60	3.64	−0.04	3.68	3.73	−0.05
4	2.88	3.39	−0.51	2.91	3.32	−0.41
5	2.37	3.12	−0.75	2.35	3.03	−0.68
6	2.02	2.87	−0.85	1.93	2.82	−0.89
rmsd				0.06	0.13	

[a] $\Delta E = \Delta E(^1B_{2u}) - \Delta E(^1B_{3u})$. [b] Reference 34.

Table 4. Contributions from Orbital Energies and K-Integrals to the Calculated Excitation Energies (eV) Using CV(∞)-TD and LDA

	calcd $^1B_{2u}$		calcd $^1B_{3u}$	
n_r[c]	$\Delta\varepsilon^a$	$(\Delta E_S - \Delta\varepsilon)^b$	$\Delta\varepsilon$	$\Delta E_S - \Delta\varepsilon$
2	3.95	0.78	4.14	0.25
3	2.83	0.85	3.55	0.18
4	2.11	0.80	3.16	0.16
5	1.60	0.75	2.90	0.13
6	1.23	0.70	2.71	0.11

[a] Orbital energy contributions to the excitation energies. [b] Contributions from K-integrals to the excitation energies. [c] Number of rings.

$\Delta\varepsilon(^1B_{2u})$. It is on the average 0.8 eV and is seen to decrease slightly with n. The magnitude of this term depends strongly on the spatial extents of a and i. If the densities of a and i are strongly overlapping the first two terms might be canceled by the last two. This has been found for some $\pi \rightarrow \pi^*$ excitation.[27] At the other extreme are charge transfer transitions[35−38] where there is no overlap and where the centers of the two densities are separated by a large distance R. In that case the two last terms reduce to $1/R$. Many studies have shown that charge transfer transitions are better described by eq 25 than by eq 26.[35−39] In the case at hand the 0.8 eV supplied by $^1/_2K_{aaaa} + {}^1/_2K_{iiii} - 2K_{aaii} + 2K_{ii\bar{a}\bar{a}}$ is just enough to bring the CV(∞)-DFT values calculated for $\Delta E(^1B_{2u})$ in line with experiment whereas the corresponding CV(2)-TD contribution given by $2K_{aiai} - K_{ii\bar{a}\bar{a}}$ is too small (0.30 eV). Given that the excitation energy for one-orbital transitions in CV(∞)-DFT is expressed by eq 10 rather than eq 11, we can in general expect it to differ from that calculated by CV(2)-TD or TDDFT irrespective of whether or not it exhibits charge transfer character.

Also shown in Table 4 and Figure 2d is $\Delta E(^1B_{3u}) - \Delta\varepsilon(^1B_{3u})$ calculated by CV(∞)-DFT for the linear acenes. It is much smaller than $\Delta E(^1B_{2u}) - \Delta\varepsilon(^1B_{2u})$ and more in line with the corresponding $\Delta E(^1B_{3u}) - \Delta\varepsilon(^1B_{3u})$ values obtained by CV(2)-TD or TDDFT, Table 2 and Figure 2b. This is consistent with that ^1L_b ($^1B_{3u}$) described by more than one orbital substitution and the fact that the energy expression 21 for CV(∞)-TD in the limit of excitations with several orbital replacements affords CV(2)-TD transition energies given by eq 23. Kuritz[19] et al. have provided an interesting analysis of how LRC functionals improve the description of the ^1L_a transitions.

We have extended our benchmark calculations also to include the 15 nonlinear acenes shown in Figure 3. The resulting singlet transition energies involving ^1L_a and ^1L_b are shown in Table 5 for TDDFT, CV(2)-TD, and CV(∞)-TD based on LDA. For ^1L_a CV(∞)-TD with a rmsd of 0.24 eV is seen to perform better than CV(2)-TD (rmsd = 0.40 eV) and especially TDDFT (0.52 eV).

dx.doi.org/10.1021/ct300372x | J. Chem. Theory Comput. 2012, 8, 4434−4440

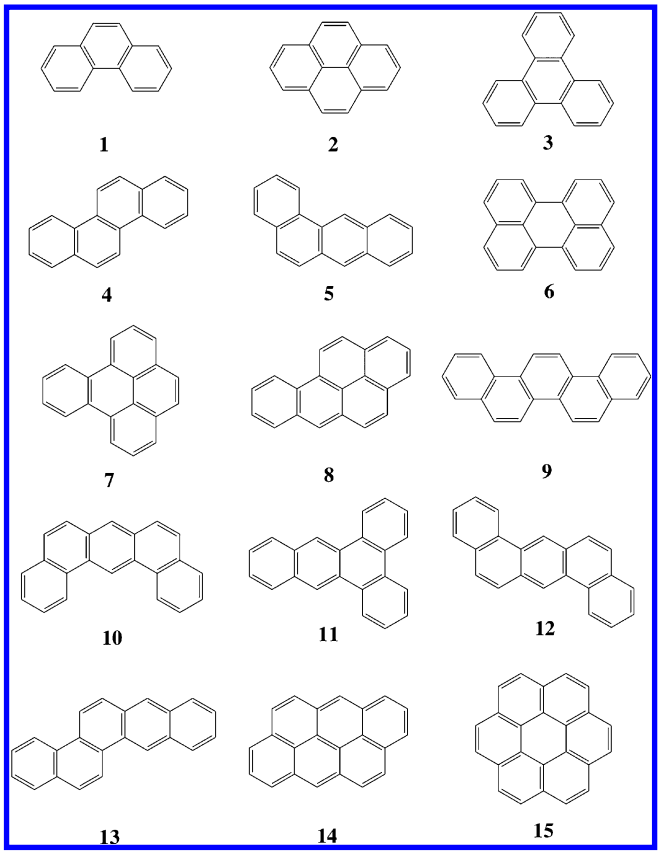

Figure 3. Structures for nonlinear acenes.

In fact, our results are of a similar quality to the best results obtained by long-range corrected (LRC) functionals.[16] We note again that the ^1L_a transitions involve a single HOMO → LUMO orbital displacement with $\eta\gamma_i = \pi/2$. For ^1L_b all three methods perform equally well with rmsd values of 0.16 eV (TDDFT), 0.15 eV(CV(2)-TD), and 0.19 eV (CV(∞)-TD), respectively. It is interesting to note that the LRC-functionals[16] in this case perform much poorer with rmsd values around 0.4 eV. Thus, CV(∞)-TD at the simple LDA level is the only scheme of the methods discussed here that gives a balanced description of $\pi \rightarrow \pi^*$ transitions involving a single orbital displacement (^1L_a) as well as a $\pi \rightarrow \pi^*$ transitions with more than one displacement.

3. CONCLUDING REMARKS

We have here tested the all order constricted variational density functional theory CV(∞)-TD in conjunction with LDA as a possible inexpensive method for the computational screening of organic dyes. Our initial test set was made up of linear polyacenes ranging from naphthalene with two to hexacene with six rings. For these systems we studied the energy difference ΔE between the excitation energies of the first two $\pi \rightarrow \pi^*$ transitions ^1L_a ($^1B_{2u}$) and ^1L_b ($^1B_{3u}$) as a function of the number of rings n_r. These systems are known to be challenging for DFT based electronic structure methods.

Our study revealed that CV(∞)-TD combined with LDA gave as accurate a description of ΔE as the sophisticated DFT/MRCI[11,12] and TDDFT/LRC[13−16] approaches for linear acenes while representing a clear improvement over TDDFT[2,3,8,9] using pure functionals or hybrids. This is interesting given the low cost and simplicity of the LDA functional and the computational efficiency of CV(∞)-TD which is a factor 2 times more expensive than TDDFT or CV(2)-TD schemes alone.

It is very well-known that transitions involving a single substitution such as ^1L_a ($^1B_{2u}$) often are better described by eq 25 that originates from the ΔSCF[39−46] energy expression than from eq 26 due to TDDFT-TD. This point has recently been demonstrated also to be the case for $\pi \rightarrow \pi^*$ transitions[27,47] in conjugated hydrocarbons. Also, Casida[48] has suggested to use eq 25 in place of eq 26 for single substitution transitions involving charge transfer as have others.[35−37] Thus, as such our CV(∞)-TD method does not bring anything new.

The novel aspect of our scheme is that it provides a seamless transition from a single substitution excitation where the ΔSCF type energy expression 25 is required to multireplacement transitions where eq 26 is appropriate. The all order constricted variation theory represents in addition a sound theoretical framework that contains both ΔSCF and adiabatic TDDFT-TD

Table 5. LDA(VWN)-Based $^1L_a(^1B_{2u})$ and $^1L_b(^1B_{3u})$ Singlet Excitation Energies (in eV) for Nonlinear Acenes with TDDFT, CV(2)-TD, and CV(∞)-TD

	^1L_a				^1L_b			
molecule[a]	TDDFT	CV(2)[b]	CV(∞)	expt[b,c]	TDDFT	CV(2)[b]	CV(∞)	expt[b,c]
1	3.88	3.99	4.09	4.24	3.59	3.61	3.74	3.76
2	3.39	3.60	3.69	3.71	3.46	3.47	3.58	3.53
3	4.16	4.27	4.41	4.54	3.74	3.76	4.00	3.89
4	3.37	3.51	3.83	3.89	3.43	3.41	3.58	3.43
5	2.96	3.16	3.98	3.63	3.10	3.07	3.68	3.22
6	2.53	2.78	2.90	2.85	3.22	3.23	3.37	
7	3.36	3.51	3.61	3.73	3.22	3.22	3.33	3.37
8	2.84	3.02	3.56	3.22	3.07	3.09	3.43	3.06
9	3.29	3.35	3.55	3.80	3.14	3.14	3.26	3.30
10	3.07	3.18	3.37	3.84	2.98	2.99	3.08	3.32
11	3.08	3.18	4.12	3.84	3.20	3.21	3.31	3.31
12	3.11	3.21	3.47	3.86	3.01	3.03	3.17	3.14
13	2.72	2.84	3.34	3.40	3.02	3.02	3.22	3.23
14	2.55	2.80	3.02	2.86	2.99	2.99	3.08	
15	3.69	3.90	3.87	3.72	3.85	3.86	3.94	
rmsd	0.52	0.40	0.24		0.16	0.15	0.19	

[a]The structures are shown in Figure 1. [b]Tamm−Dancoff approximation. [c]The experimental values are taken from ref 2.

dx.doi.org/10.1021/ct300372x | J. Chem. Theory Comput. 2012, 8, 4434−4440

as special cases. We should finally note that that the CV(∞)-TD scheme is a simple form of more refined theories such as SCF-CV(∞)-DFT[27] in which **U** is optimized with respect to $E[\rho^{(n)+}, \rho^{(n)-}]$ rather than $E[\rho^{(2)+}, \rho^{(2)-}]$ and R-CV(∞)-DFT or RSCF-CV(∞)-DFT in which we also introduce relaxation of the orbitals not participating directly in the excitation.[29] However, in spite of its simplicity the CV(∞)-TD scheme was shown recently to afford an average deviation from experiment of approximately 0.3 eV for both semilocal and hybrid functionals in an extensive study of $\pi \rightarrow \pi^*$ transitions[27,47] involving conjugated hydrocarbons. The current study on linear acenes adds further to the notion that CV(∞)-TD might be a useful and cost efficient supplement to TDDFT in the study of dyes. We have in addition provided an extensive theoretical analysis of how CV(∞)-TD complement TDDFT.

AUTHOR INFORMATION

Corresponding Author

*E-mail mkrykuno@ucalgary.ca.

Notes

The authors declare no competing financial interest.

ACKNOWLEDGMENTS

This work was supported by NSERC. The computational resources of WESTGRID were used for all calculations. T.Z. thanks the Canadian Government for a Canada Research Chair and the Humboldt foundation for a generous award.

REFERENCES

(1) Platt, J. R. *J. Chem. Phys.* **1949**, *17*, 484−496.
(2) Grimme, S.; Parac, M. *ChemPhysChem* **2003**, *4*, 292−295.
(3) Parac, M.; Grimme, S. *Chem. Phys.* **2003**, *292*, 11−21.
(4) Casida, M. E. In *Recent Advances in Density Functional Methods*; Chong, D. P., Ed.; World Scientific: Singapore, 1995; Vol. *1*, pp 155−192.
(5) Gross, E. K. U.; Dobson, J. F.; Petersilka, M. *Top. Curr. Chem.* **1996**, *181*, 81−172.
(6) Bauernschmitt, R.; Ahlrichs, R. *Chem. Phys. Lett.* **1996**, *256*, 454−464.
(7) *Time-Dependent Density Functional Theory, Lecture Notes Physics 706*; Marques, M. A. L., Ulrich, C. A., Nagueira, F., Rubio, A., Burke, K., Gross, E. K. U., Eds.; Springer: Berlin, 2006.
(8) Jacquemin, D.; Wathelet, V.; Perpete, E. A.; Adamo, C. *J. Chem. Theory Comput.* **2009**, *5*, 2420−2435.
(9) Goerigk, L.; Grimme, S. *J. Chem. Phys.* **2010**, *132*, 184103.
(10) Dierksen, M.; Grimme, S. *J. Phys. Chem. A* **2004**, *108*, 10225−10237.
(11) Grimme, S.; Waletzke, M. *J. Chem. Phys.* **1999**, *111*, 5645−5655.
(12) Marian, C.; Gilka, N. *J. Chem. Theory Comput.* **2008**, *4*, 1501−1515.
(13) Jacquemin, D.; Perpete, E. A.; Scuseria, G. E.; Ciofni, I.; Adamo, C. *J. Chem. Theory Comput.* **2008**, *4*, 123−135.
(14) Jacquemin, D.; Perpete, E. A.; Ciofni, I.; Adamo, C. *Theor. Chem. Acc.* **2011**, *128*, 127−136.
(15) Wong, B. M.; Hsieh, T. H. *J. Chem. Theory Comput.* **2010**, *6*, 3704−3712.
(16) Richard, R. M.; Herbert, J. M. *J. Chem. Theory Comput.* **2011**, *7*, 1296−1306.
(17) Stein, T.; Kronik, L.; Baer, R. *J. Am. Chem. Soc.* **2009**, *131*, 2818−2820.
(18) Stein, T.; Kronik, L.; Baer, R. *J. Chem. Phys.* **2009**, *131*, 244119.
(19) Kuritz, N.; Stein, T.; Kronik, R. B. L. *J. Chem. Theory Comput.* **2011**, *7*, 2408−2415.
(20) Grimme, S.; Neese, F. *J. Chem. Phys.* **2007**, *127*, 154116.
(21) Grimme, S. *J. Chem. Phys.* **2006**, *124*, 034108.
(22) Karton, A.; Tarnopolsky, A.; Lamere, J. F.; Schatz, G. C.; Martin, J. M. L. *J. Phys. Chem. A* **2008**, *112*, 12868−12886.
(23) Goerigk, L.; Moellmann, J.; Grimme, S. *Phys. Chem. Chem. Phys.* **2009**, *11*, 4611−4620.
(24) Goerigk, L.; Grimme, S. *J. Phys. Chem. A* **2009**, *113*, 767−776.
(25) Goerigk, L.; Grimme, S. *J. Chem. Theory Comput.* **2011**, *7*, 3272−3277.
(26) Head-Gordon, M.; Rico, R. J.; Oumi, M.; Lee, T. *J. Chem. Phys. Lett.* **1994**, *219*, 21−29.
(27) Ziegler, T.; Krykunov, M.; Cullen, J. *J. Chem. Phys.* **2012**, *136*, 124107.
(28) Hirata, S; Head-Gordon, M. *Chem. Phys. Lett.* **1999**, *314*, 291−299.
(29) Ziegler, T; Krykunov, M. *J. Chem. Phys.* **2010**, *133*, 074104.
(30) te Velde, G.; Bickelhaupt, F. M.; van Gisbergen, S. J. A.; Fonseca Guerra, C.; Baerends, E. J.; Snijders, J. G.; Ziegler, T. *J. Comput. Chem.* **2001**, *22*, 931−967.
(31) Van Lenthe, E.; Baerends, E. J. *J. Comput. Chem.* **2003**, *24*, 1142−1156.
(32) Vosko, S. H.; Wilk, L.; Nusair, M. *Can. J. Phys.* **1980**, *58*, 1200−1211.
(33) Krykunov, M.; Ziegler, T.; van Lenthe, E. *J. Phys. Chem. A* **2009**, *113*, 11495−11500.
(34) Biermann, B.; Schmidt, W. *J. Am. Chem. Soc.* **1980**, *102*, 3163−3173.
(35) Ziegler, T.; Seth, M.; Krykunov, M.; Autschbach, J.; Wang, F. *THEOCHEM* **2009**, *914*, 106−109.
(36) Ziegler, T.; Seth, M.; Krykunov, M.; Autschbach, J. *J. Chem. Phys.* **2008**, *129*, 184114.
(37) Ziegler, T.; Seth, M.; Krykunov, M.; Autschbach, J.; Wang, F. *J. Chem. Phys.* **2009**, *130*, 154102.
(38) Cullen, J.; Krykunov, M.; Ziegler, T. *Chem. Phys.* **2011**, *391*, 11−18.
(39) Ziegler, T.; Rauk, A.; Baerends, E. J. *Chem. Phys.* **1976**, *16*, 209−217.
(40) Slater, J. C.; Wood, J. H. *Int. J. Quantum Chem.* **1971**, *Suppl. 4*, 3−34.
(41) Slater, J. C. *Adv. Quantum Chem.* **1972**, *6*, 1−31.
(42) Ziegler, T.; Rauk, A.; Baerends, E. J. *Theor. Chim. Acta* **1977**, *43*, 261−271.
(43) Levy, M.; Perdew, J. P. *Phys. Rev.* **1985**, *A 32*, 2010−2021.
(44) Nagy, A. *Phys. Rev. A* **1996**, *53*, 3660−3663.
(45) Besley, N.; Gilbert, A.; Gill, P. *J. Chem. Phys.* **2009**, *130*, 124308.
(46) Gavnholt, J.; Olsen, T.; Engelund, M.; Schiotz, J. *Phys. Rev. B* **2008**, *78*, 075441.
(47) Kowalczyk, T.; Yost, S. R.; Van Voorhis, T. *J. Chem. Phys.* **2011**, *134*, 054128.
(48) Cassida, M. E.; Gutierrez, F.; Guan, J.; Gadea, F.-X.; Salahub, D.; Daudey, J.-P. *J. Chem. Phys.* **2000**, *113*, 7062−7071.
(49) Amos, A. T.; Hall, G. G. *Proc. R. Soc.* **1961**, *A263*, 483−493.
(50) Martin, R. L. *J. Chem. Phys.* **2003**, *118*, 4775−4777.